Scientific Research Publishing

Journal of Power and Energy Engineering, 2024, 12, 60-75
https://www.scirp.org/journal/jpee
ISSN Online: 2327-5901
ISSN Print: 2327-588X

Mitigation of Transients in Capacitor Coupled Substations Using Traditional RLC Filter Techniques

Sinqobile Wiseman Nene, Bolanle Tolulope Abe, Agha Francis Nnachi

Department of Electrical Engineering, Tshwane University of Technology, eMalahleni, South Africa
Email: wnene@hailienene.com, AbeBT@tut.ac.za, NnachiAF@tut.ac.za

How to cite this paper: Nene, S.W., Abe, B.T. and Nnachi, A.F. (2024) Mitigation of Transients in Capacitor Coupled Substations Using Traditional RLC Filter Techniques. *Journal of Power and Energy Engineering*, **12**, 60-75.
https://doi.org/10.4236/jpee.2024.125003

Received: April 10, 2024
Accepted: May 28, 2024
Published: May 31, 2024

Abstract

This article presents an extensive examination and modeling of Capacitor Coupled Substations (CCS), noting some of their inherent constraints. The underlying implementation of a CCS is to supply electricity directly from high-voltage (HV) transmission lines to low-voltage (LV) consumers through coupling capacitors and is said to be cost-effective as compared to conventional distribution networks. However, the functionality of such substations is susceptible to various transient phenomena, including ferroresonance and overvoltage occurrences. To address these challenges, the study uses simulations to evaluate the effectiveness of conventional resistor-inductor-capacitor (RLC) filter in mitigating hazardous overvoltage resulting from transients. The proposed methodology entails using standard RLC filter to suppress transients and its associated overvoltage risks. Through a series of MATLAB/Simulink simulations, the research emphasizes the practical effectiveness of this technique. The study examines the impact of transients under varied operational scenarios, including no-load switching conditions, temporary short-circuits, and load on/off events. The primary aim of the article is to assess the viability of using an established technology to manage system instabilities upon the energization of a CCS under no-load circumstances or in case of a short-circuit fault occurring on the primary side of the CCS distribution transformer. The findings underscore the effectiveness of conventional RLC filters in suppressing transients induced by the CCS no-load switching.

Keywords

Capacitor Coupled Substation, System Modeling, Ferroresonance, RLC filters, Power Electronics, Transients, Capacitor Voltage Transformers, Transmission Lines

1. Introduction

The foundational concepts of Capacitor Coupled Substations (CCS) have been firmly established and extensively explored in recent years [1] [2] [3]. The core operational principle of a CCS is based on traditional capacitor voltage transformers (CVT), commonly used for measurement and protective functions within power utility systems [4]. A CVT employs a capacitor divider to reduce transmission HV to levels suitable for measurement [5]. Although the capacitor divider concept has been recognized for some time, its recent application in transforming high voltage (HV) to medium voltage (MV) for power delivery has brought new challenges [6]. Designing a CCS requires addressing phenomena like transients and ferroresonance, which historically posed challenges in substation design. Ferroresonance in electric circuits occurs when a nonlinear inductance circuit is supplied from a source with series capacitance and the circuit subjected to disturbances caused by the opening and closing of the system circuit breakers [7] [8]. Ferroresonance can also be defined as a complex nonlinear electrical phenomenon that can lead to thermal and insulation failures in transmission and distribution systems [9] [10]. This phenomenon may result in overvoltage and over current which may result in the power system network components damage [11].

A CCS is designed to directly supply electricity from HV transmission lines to MV systems, which is said to offer substantial cost advantages over conventional distribution networks. However, transient issues such as ferroresonance and overvoltage can cause damages in these substations [12]. This study focuses on the impact of transients during the specifically selected operating conditions.

The objective of this article is to develop a capacitor coupled substation integrating an efficient method to mitigate transients using conventional RLC filters. This objective is realized through the integration of conventional ferroresonance suppression circuit (FSC) on the secondary side of the CCS distribution transformer. The system is modelled and simulated on MATLAB/Simulink under no-load switching, ON and OFF switching and short-circuit fault applied to the primary side of the distribution transformer. The details of the model and simulation are detailed in the sections that follow. This study contributes to the knowledge body of the CCS behaviour during specific operations in order to understand and/or determine the impact on the downstream of the CCS.

2. Background Theory

The ferroresonance phenomenon involves multiple modes with different frequencies, such as the fundamental frequency, sub-harmonic, quasi-periodic, and chaotic modes [13]. When a sudden transition between steady states occurs due to disturbances, switching actions, or gradual shifts in parameter values, ferroresonance can trigger overvoltage and overcurrent in power networks, posing a risk of damage to transformers and significant harm to network devices such as series capacitors [14]. Unlike resonance in circuits with linear capacitances and inductances, ferroresonance mainly occurs in circuits with nonlinear inductance due to the transformer core behaviour [15]. The magnetic core of the transformer is considered a nonlinear inductance, while line-to-line, line-to-earth capacitances, series capacitors, and grading capacitors of circuit breakers are considered linear capacitances [16].

Ferroresonance oscillations depend not only on frequency but also on factors such as system voltage magnitude, initial magnetic flux condition of the transformer iron core, total core losses in the circuit, and the switching moment intervals. CCS is also susceptible to ferroresonance [17].

2.1. Capacitor Coupled Substation (CCS)

Although the principle of operation of a CCS is derived from a CVT, CVTs are commonly utilized in transmission substations for metering and protection purposes, therefore, their load burden is low and limited [18] [19]. A simplified representation of a 400 kV/11 kV CCS selected for this study is shown on **Figure 1**. A 400 kV/11 kV CCS implies that the transmission HV is at 400 kVrms level while the tap-voltage or primary side of the distribution transformer is at 11 kVrms.

In **Figure 1**, the schematic representation of the CCS equivalent circuit is presented. Bus A represents the upstream supply side of the HV transmission network, Bus B, represents the downstream of the HV transmission network and Bus C represents the CCS tap-voltage feeding the distribution network transformer. From **Figure 1**, a Thevenin equivalent of the voltage divider (C1 and C2) is shown, with the Thevenin equivalent voltage represented as per (1) and its impedance is that of capacitors C1 and C2 as shown on (2).

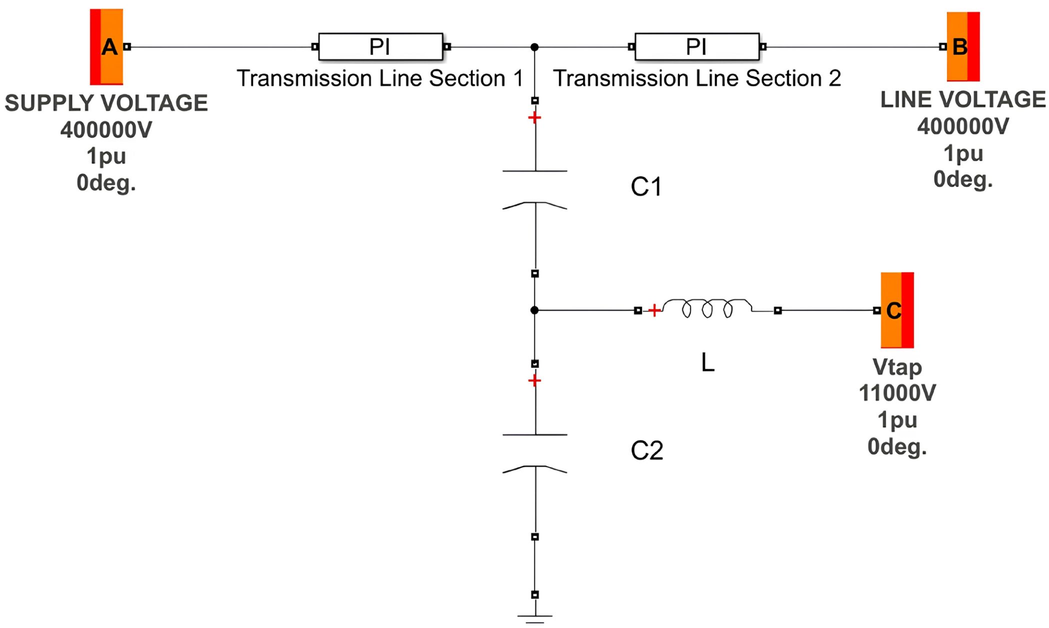

Figure 1. Simplified CCS.

$$V\_th = V\_in \times C\_1/((C\_1 + C\_2)) \quad (1)$$

$$C\_th = C\_1 + C\_2 \quad (2)$$

The formulae, (1) and (2), serve as the basis for element calculation in a CCS. The objective is to ensure that the Vout remains stable as it feeds into a downstream transformer for the distribution system. From **Figure 1**, there is also a compensating reactor (L). The reactor is used for voltage regulation. The reactor is chosen based on considerations of various factors, including feeder characteristics, transformer specifications, and the reactance and resistance of both the load and the reactor [20].

2.2. Ferroresonance Suppression Circuit (FSC)

The ferroresonance suppression circuit (FSC) is used to prevent damages due to ferroresonance in an electrical system [21]. A simplified representation of a CCS with FSC is shown in **Figure 2**.

Figure 2 shows the FSC connected to a CCS. The inductor (L), connected to the capacitive voltage divider is used to cancel the Thevenin impedance at 50 Hz and this is achieved by adjusting energy storage components such as they satisfy the concept represented by (3):

$$LC\omega \wedge 2 = 1 \quad (3)$$

where: $\omega = 2\pi 50$ for a 50 Hz system.

Satisfaction of (3) results in the output voltage being in-phase with the tap-voltage and the supply voltage. The inductor (L) is thus given by (4).

$$L = 1/(\omega \wedge 2 \times C\_TH) \quad (4)$$

There are two main types of damping circuit operational modes; active ferroresonance suppression circuit (AFSC) and passive ferroresonance suppression circuit (PFSC).

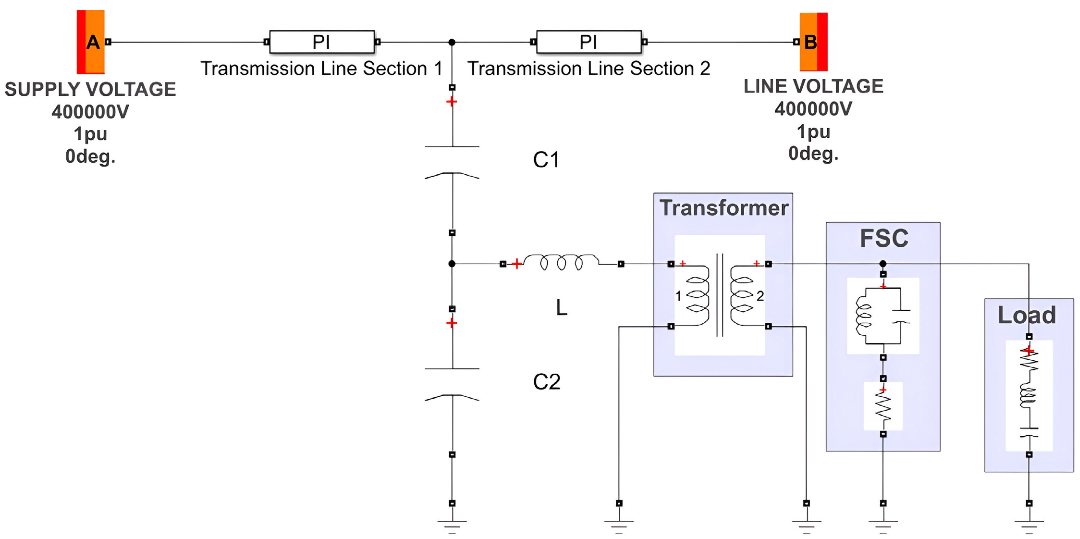

Figure 2. CCS with FSC.

2.2.1. FSC Active Operational Mode

In an actively operational mode, the FSC include capacitors (C), resistors (R), and iron core inductors (L) that are connected and tuned to the fundamental frequency. These elements are permanently integrated on the secondary side of a system transformer and impact the transient response of a CCS [22]. This parallel-connected filter is strategically implemented to address both ferroresonance and harmonic transients within the system. Operating as an open-circuit at the fundamental frequency, it transforms into a short-circuit, incorporating losses, at frequencies other than the fundamental. The inclusion of resistive losses plays a crucial role in effectively mitigating hazardous transients within the system [23].

2.2.2. FSC Passive Operational Mode

In a passive operational mode, the FSC consists of a power electronic control circuit in series with a resistor. This circuit activates in response to overvoltage events. Power electronic devices are employed to selectively switch a damping resistor to the secondary side of the transformer as required [24].

2.3. RLC-Filter Design

Figure 3 shows the different configurations of an RLC-filter design.

Figure 3(a) shows the schematic of a serial-parallel RLC filter, where a capacitor is connected in parallel with an iron core inductor tuned for the fundamental frequency. The resistor (R) functions as a damping resistor strategically engineered to suppress ferroresonance oscillations within a single cycle. The circuit is tuned with a high factor to effectively suppress ferroresonance oscillations at frequencies other than the fundamental frequency.

The FSC can also be represented using two distinct models. In one model (**Figure 3(b)**), the FSC is characterized with an air core inductance. Alternatively, it can be portrayed as a non-saturable transformer, as shown in **Figure 3(c)**. In **Figure 3(c)** model, primary and secondary windings are connected with specified polarities. The computed value is integrated into the transformer model as a self-inductance, ensuring parallel resonance at the fundamental frequency. At frequencies other than the fundamental, only the leakage inductance comes into play, with the damping resistor responsible for reducing ferroresonance oscillations.

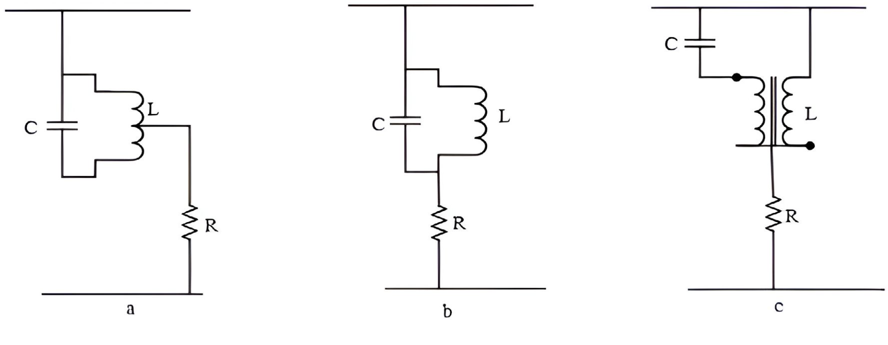

Figure 3. FSC Filter Design.

3. Methodology

A 400 kV/11 kV CCS with known parameters was developed using MATLAB/Simulink software. The model was executed and the system behaviour analysed. The main focus was on the primary and secondary sides of the distribution transformer during disturbances which were represented by switching the system ON and OFF at no-load. The system was then switched ON and OFF with a three-phase fault on the primary side of the transformer. In both operations, the interference/transient phenomenon was observed.

Subsequently, the model underwent simulation using a standard RLC filter, and once more, the behaviour of the system was observed. The simulation parameters for the CCS model used are presented on Table 1.

The parameters on Table 1 were used on the MATLAB/Simulink model presented on Figure 4.

Table 1. CCS Model Parameters.

Parameter	Description
V_s	Selected Tx Line
V_T	Selected Tap Voltage
CCS Load	Selected load value
Downstream Load	Selected load value
CCS Transformer	Selected Transformer
C_1	Capacitor 1
C_2	Capacitor 2
L	Line Inductance
Tx Line Section #1	Selected
Tx Line Section #2	Selected

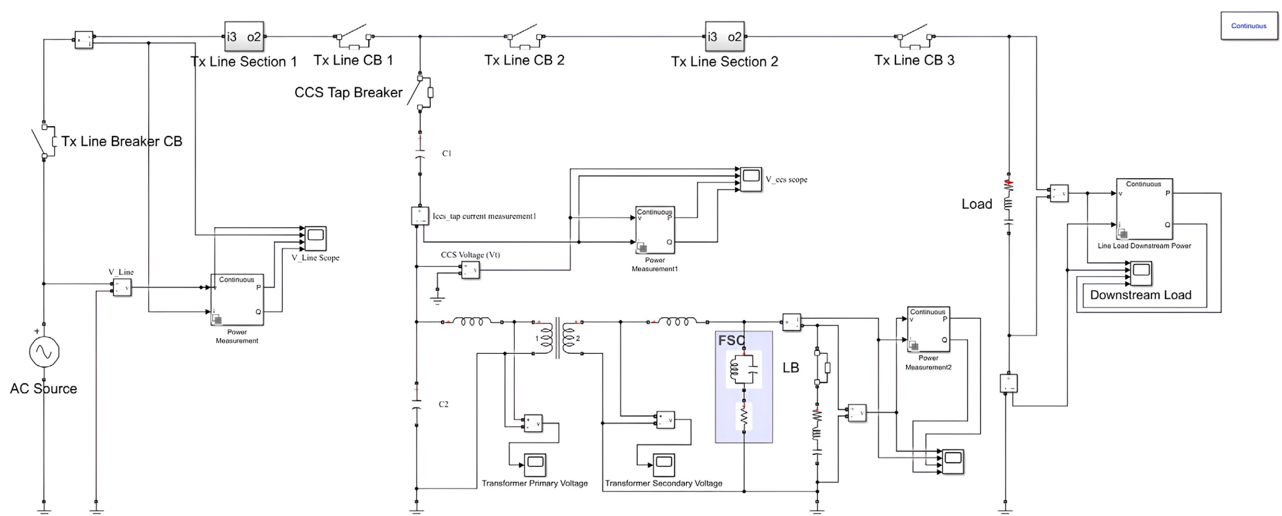

Figure 4. Full CCS Model with FSC.

The MATLAB/Simulink model depicted in Figure 4 was employed to simulate the system, initially without the FSC incorporated into the circuit, and subsequently with the FSC included in the circuit. The results are presented on the figures in the following section. The interference was initially introduced by switching ON and OFF the CCS circuit breaker, and by simulating a three-phase fault within the primary side of the CCS distribution transformer. All results were observed during system switching under no-load conditions. All simulations were conducted using identical switching times. These times are presented on Table 2.

The times presented on Table 2 are for the CCS breaker operations. In the simulation, all line breakers closed immediately upon initiation, while the load breaker (LB) opened simultaneously to depict a no-load system. The results and discussions are discussed below. The simulation is based on a 400kV/11kV CCS with parameters as presented on Table 3 and the supply or transmission line parameters represented in Figure 5.

4. Results and Discussions

Utilizing the model depicted in Figure 4 from the previous section, the graphical representation of the voltage response of the primary side of the distribution transformer is presented in Figure 6 and Figure 7.

Table 2. CCS circuit breaker switching.

CCS Circuit Breaker Position	*Time* (s)
Close	0.2
Open	0.4
Close	0.6
Open	0.8
Close	1

Table 3. Model parameters.

Parameter	Value
Supply	400 kVrms, 50 Hz
Transmission line section 1 and 2	300 km, 0.01273 Ω/km, 0.9337 mH/km, 0.01274 μF/km
Transmission line load	50 MW @ 400 kV, 50 Hz
CCS C_1	0.09 πF
CCS C_2	7.5 μF
L_1 and L_2	1 mH
Distribution Transformer	100 kVA, 50 Hz, 11 kV/400 V, 0.002 Rpu, 0.08 Lpu
CCS Load	80 kW @400 V, 50 Hz, 100 Ql, 100 Qc
FSC	L = 1 mH, C = 1 μF, R = 1 Ω

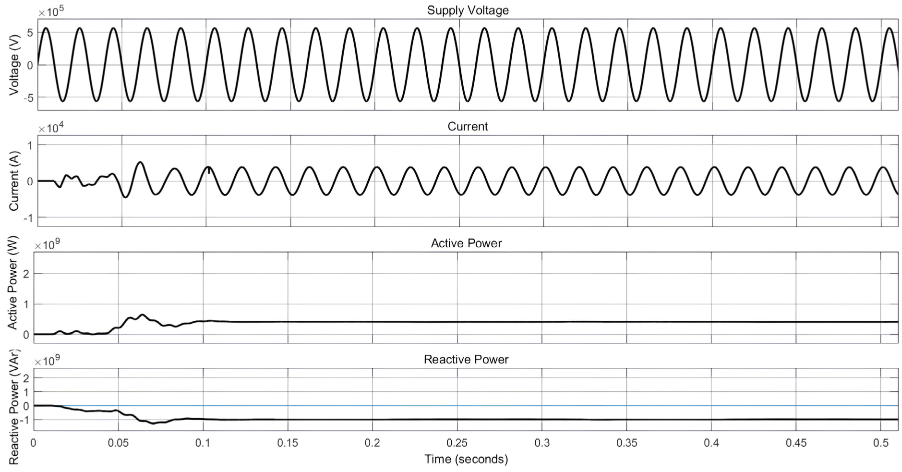

Figure 5. System supply parameters.

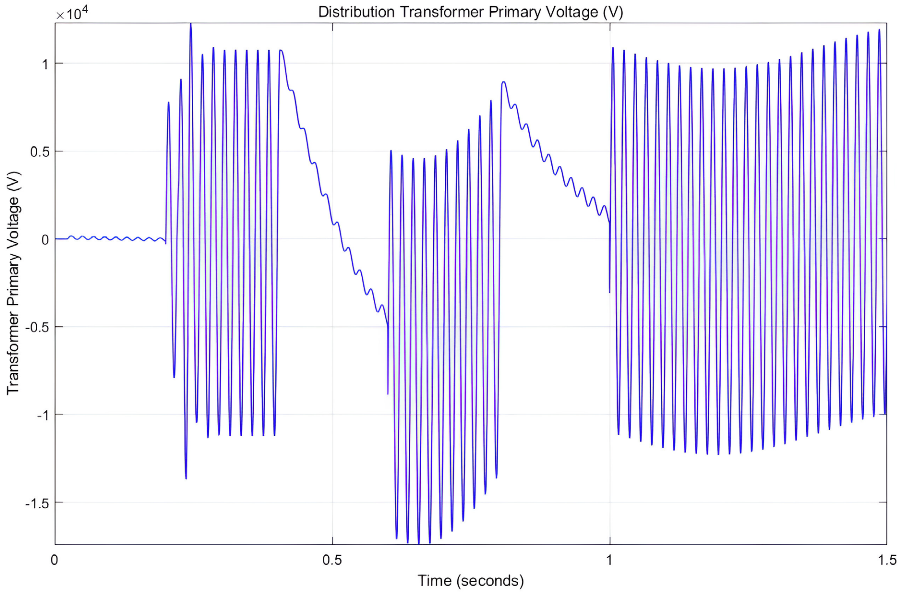

Figure 6. Distribution transformer primary voltage without FSC.

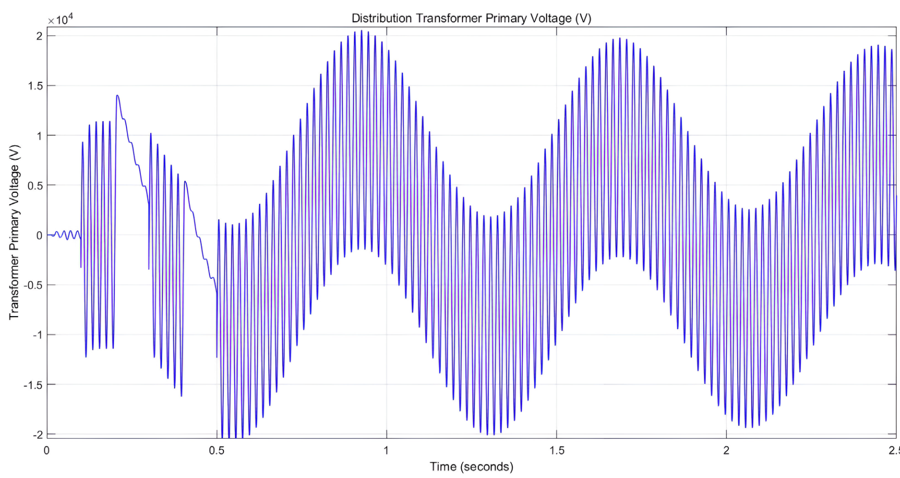

Figure 7. Distribution transformer primary voltage without FSC_expanded duration.

The results shown in **Figure 6** and **Figure 7** are derived from executing the model illustrated in **Figure 4** from the preceding section. **Figure 6** and **Figure 7** provide simulation results of the primary side of the CCS distribution transformer voltage response, while **Figure 8** and **Figure 9** illustrate the corresponding secondary voltage of the CCS distribution transformer.

In the South African context, this voltage is used for single-phase household supply by utilizing one line alongside the neutral or ground point, effectively converting 400 V three-phase voltage to 230 V single-phase voltage, where phase voltage ($V\varphi$)equals toline voltage (VLL) divided by square-root-of-3.

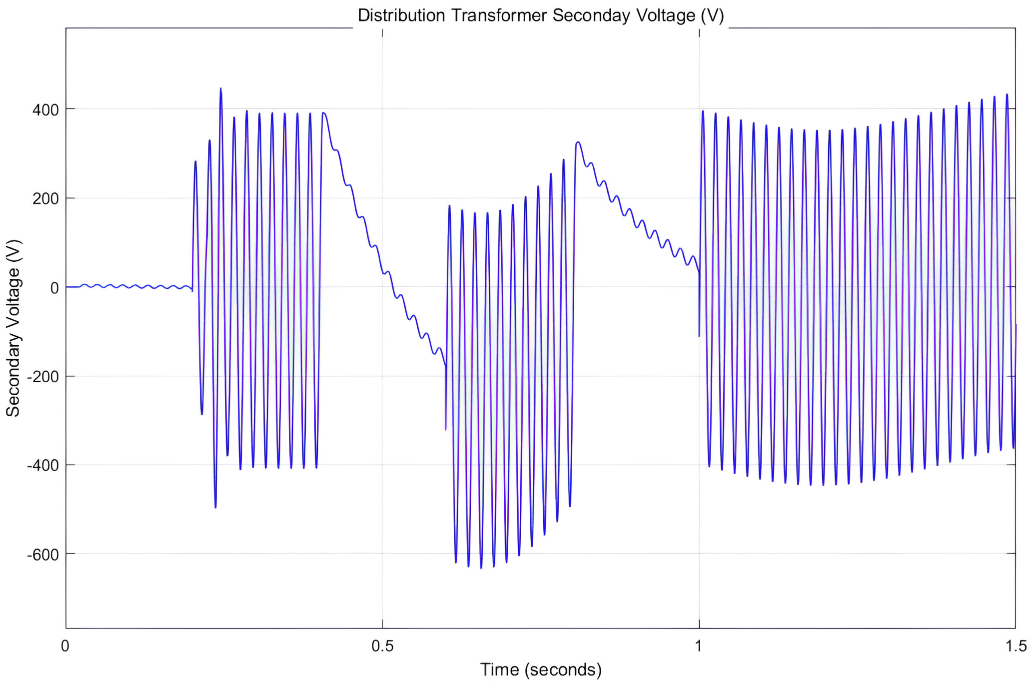

Figure 8. Distribution transformer secondary voltage without FSC.

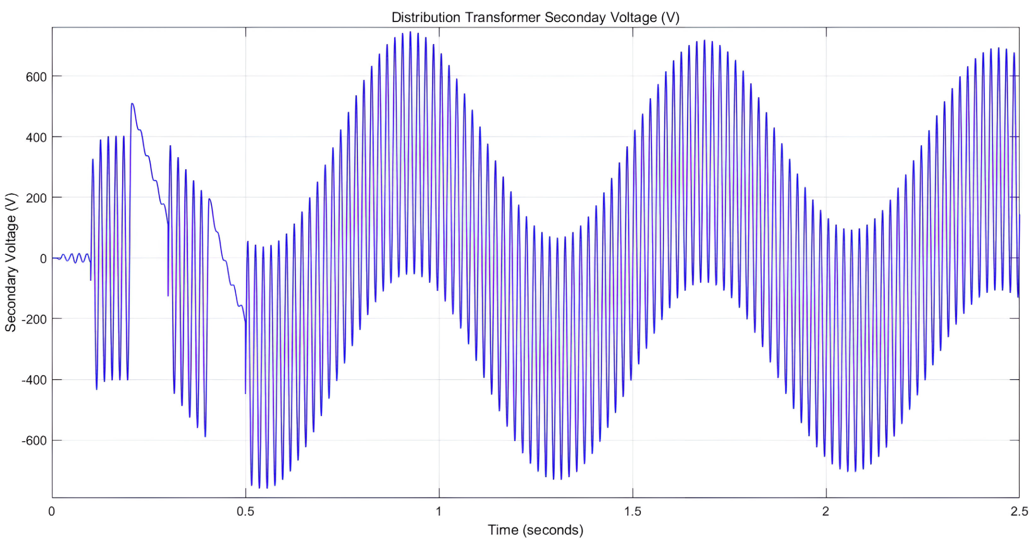

Figure 9. Distribution transformer secondary voltage without FSC_expanded duration.

Figure 6, Figure 7, Figure 8 and Figure 9 present the primary and secondary voltage representations during the switching of the system under no-load conditions. It is evident that in the absence of any form of a FSC, the voltage exhibits instability and resonance. Upon each activation or deactivation of the system, a considerable amount of time is required for stabilization. Without the FSC, the voltage remains in oscillation, emphasizing the crucial role of the FSC in ensuring stability.

Upon connecting the FSC to the secondary side of the CCS distribution transformer and repeating the same switching operation, the resulting waveforms are illustrated in Figure 10 and Figure 11, representing the primary and secondary sides, respectively.

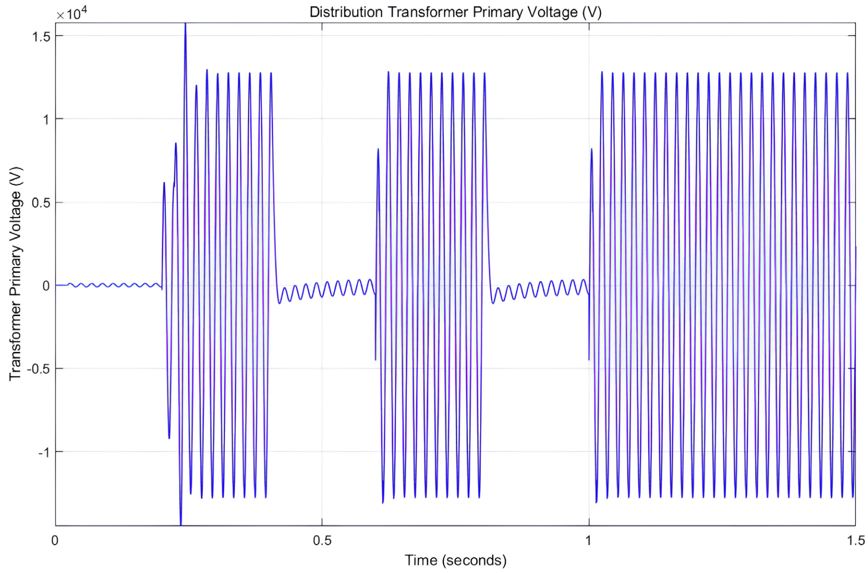

Figure 10. Distribution transformer primary voltage with FSC.

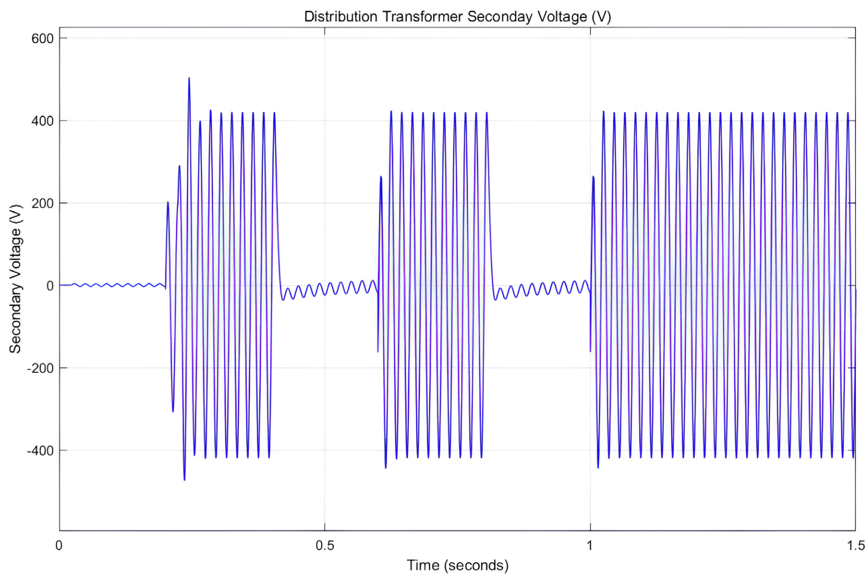

Figure 11. Distribution transformer secondary voltage with FSC.

The identical operation, with and without the FSC, was repeated while a three-phase short-circuit fault was applied on the primary side of the CCS distribution transformer. The results are presented in Figure 12, Figure 13, Figure 14 and Figure 15 for the system with the FSC connected.

As evident from Figure 10 and Figure 11, the addition of a FSC stabilizes both the primary and the secondary voltages immediately after the switching operation.

When the fault is applied, the results are as shown in Figure 12, Figure 13, Figure 14 and Figure 15.

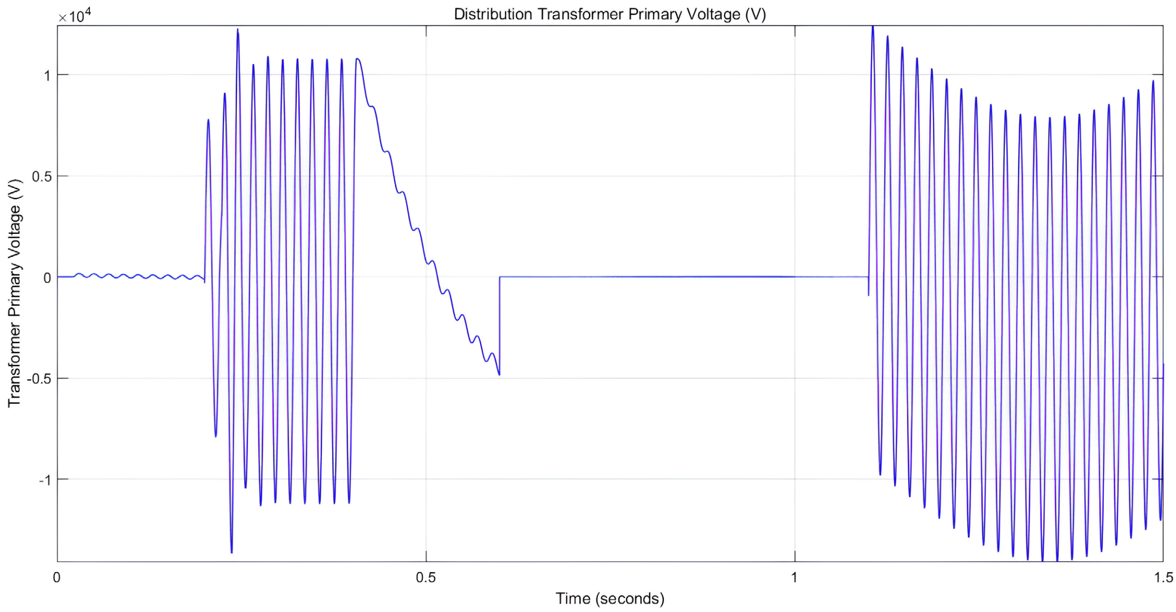

Figure 12. Transformer primary voltage with fault without FSC.

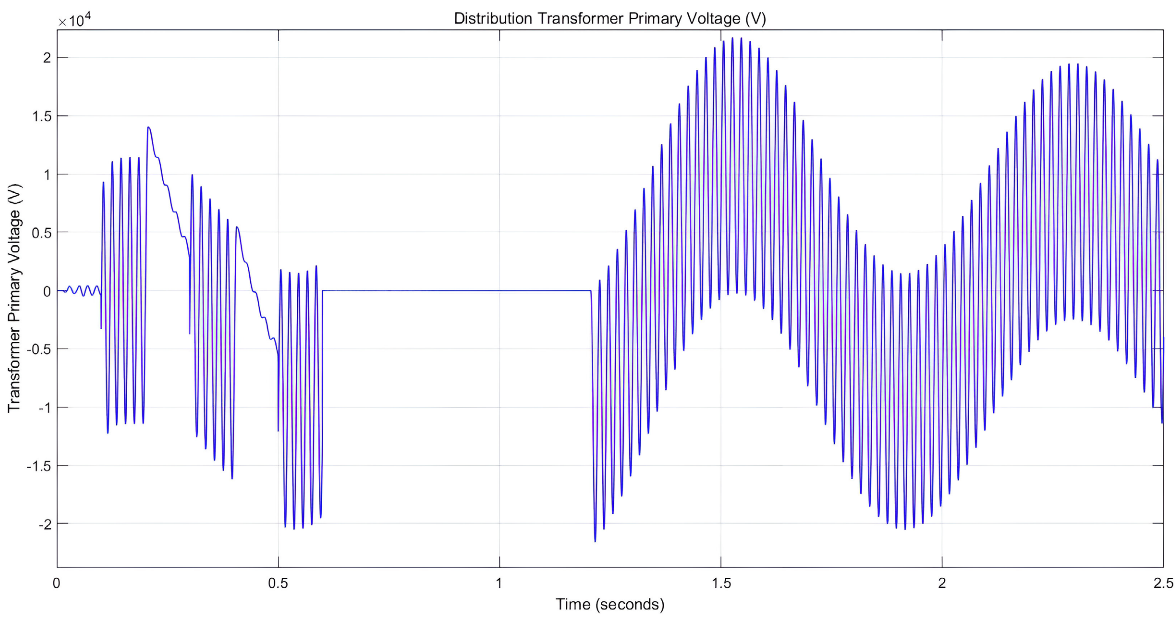

Figure 13. Transformer primary voltage with fault without FSC_Expanded.

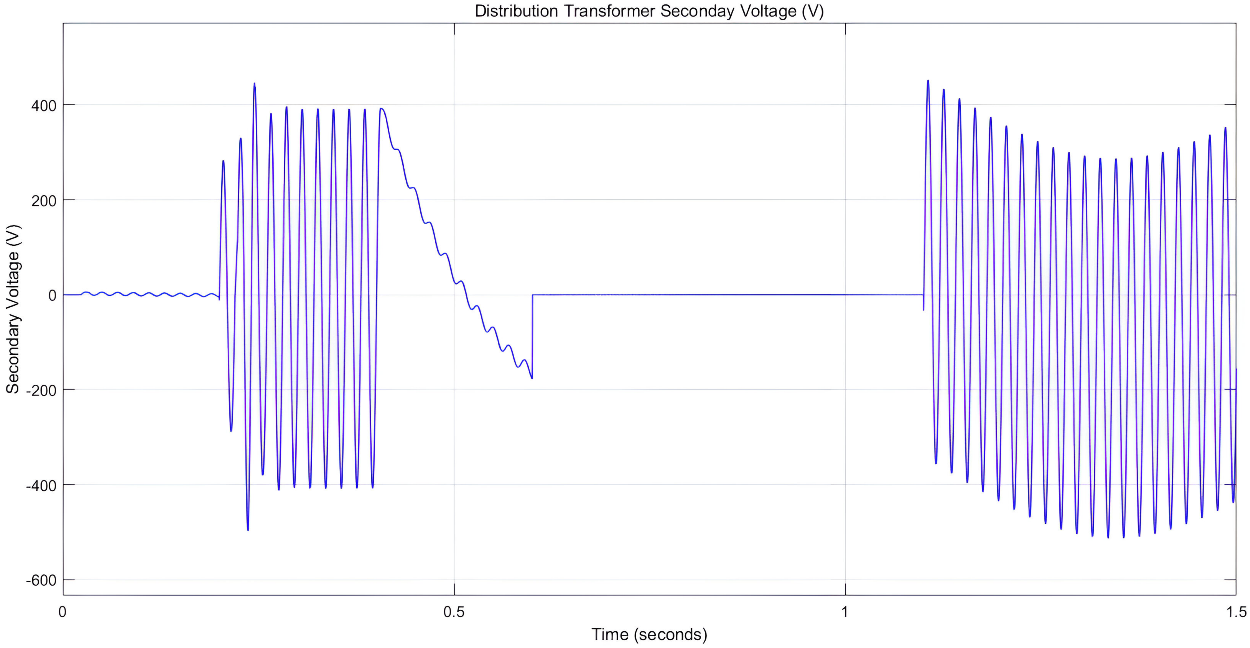

Figure 14. Transformer secondary voltage with fault, without FSC.

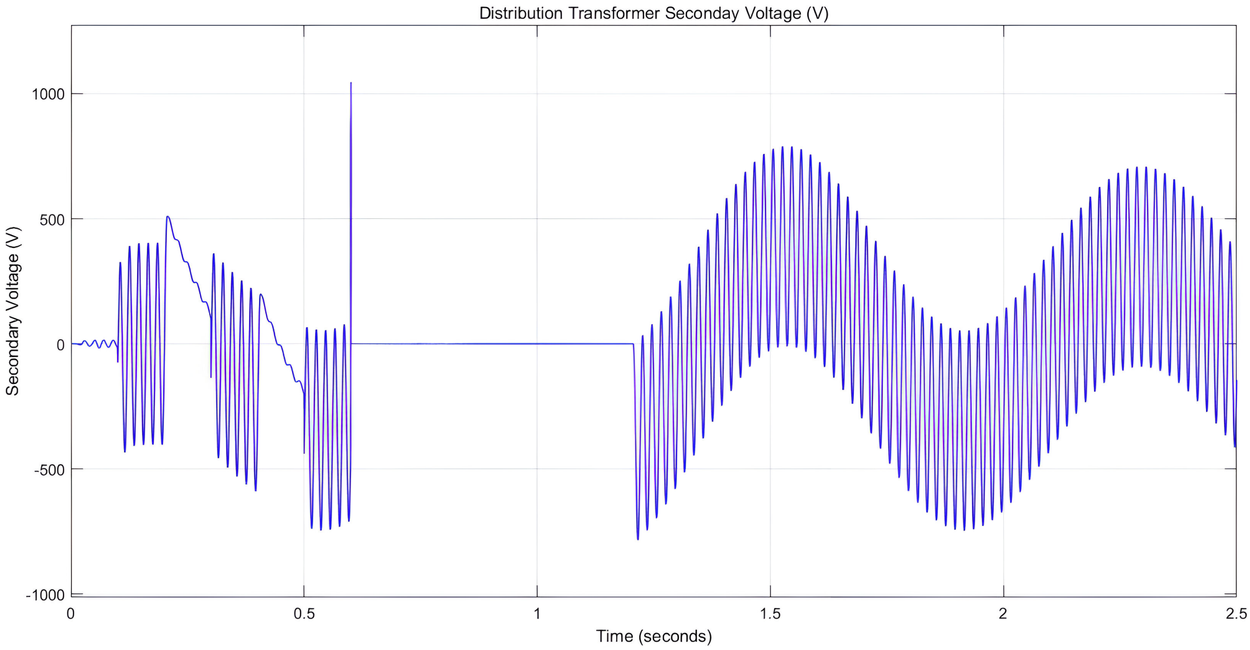

Figure 15. Transformer secondary voltage with fault, without FSC (extended simulation time).

With the same switching durations, the FSC significantly contributes to rapidly stabilizing the system once the fault has been cleared during switching operations. This phenomenon is depicted in Figure 16 and Figure 17, showing the system's rapid stabilization after clearing the fault condition. The incorporation of the FSC ensures a seamless transition to standard operating parameters, effectively alleviating any potential instabilities that could otherwise emerge for the transients results.

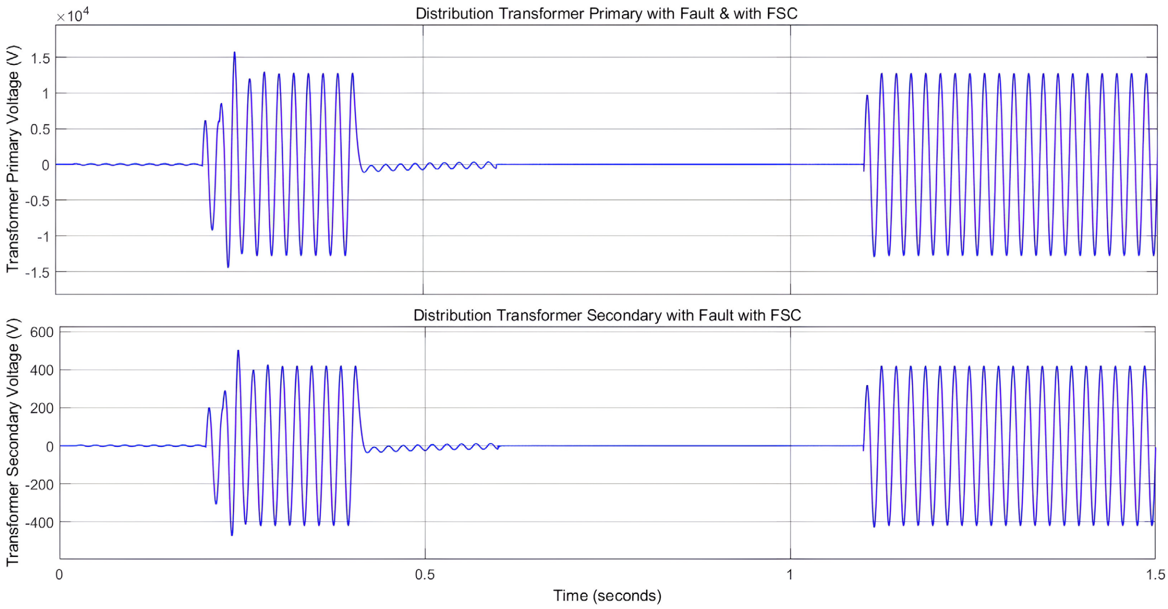

Figure 16. Transformer voltage with fault with FSC.

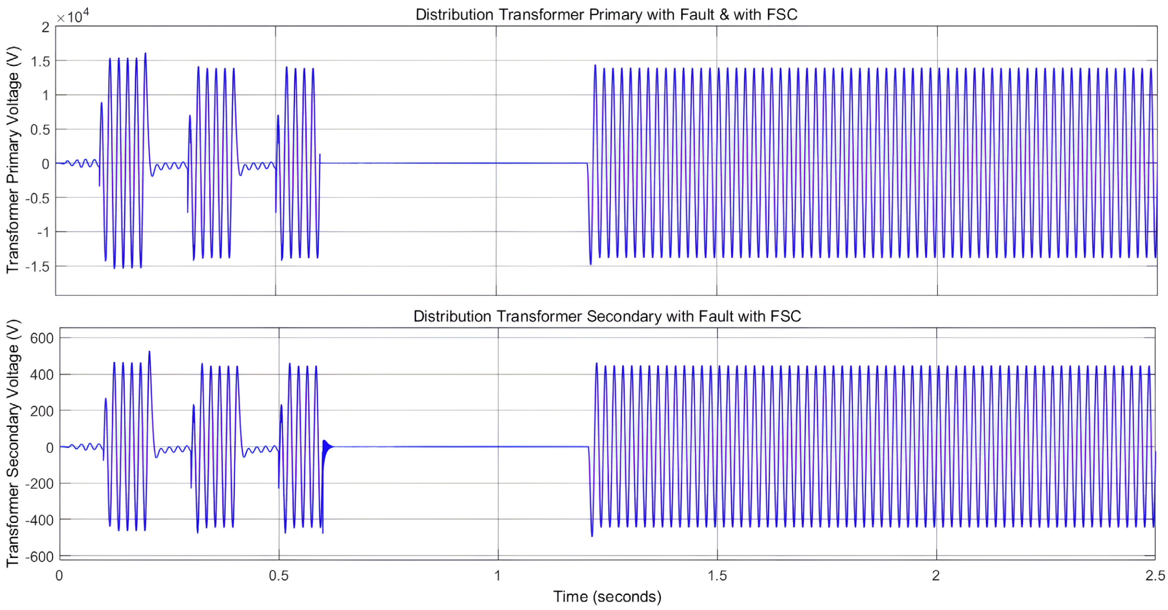

Figure 17. Transformer voltage with fault with FSC_Expanded.

Despite **Figure 15** and **Figure 17** depicting distinct switching operations, the results achieved consistently demonstrate that the FSC effectively stabilizes any oscillations when integrated into the circuit.

Hence, it is reasonable to affirm that a conventional FSC can be incorporated in the design of a CCS. This FSC serves to mitigate voltage oscillations during both switching operations and after the clearance of a fault. The outcomes indicate that the FSC facilitates the system in sustaining the desired primary and secondary voltages at 11 kV and 400 V, respectively, following both the switching operation and fault clearance.

5. Conclusions

The Capacitor Coupled Substation (CCS) offers an alternative approach to delivering electrical power directly from HV transmission lines to MV systems. This method circumvents the requirement for conventional distribution infrastructure. While the study examines distinct limitations inherent to the CCS system, a particular emphasis on voltage stability and its implications on the main transmission network were the main points of interest. The results of this study reveal two significant observations: firstly, the integration of a CCS does not exert any negative influence on the voltage of the upstream system of the transmission network; secondly, conventional technologies demonstrate proficiency in preserving the stability of the voltage on the CCS load side, notwithstanding potential disturbances such as ferroresonance resulting from switching operations, no-load switching, and system fault.

Therefore, it is reasonable to conclude that a simple RLC-based FSC can effectively ensure voltage system stability, negating the need for overly sophisticated electronic components.

As this study forms part of the proposed novel concept of Capacitor Coupled Substation with Controllable Network Transformer (CCS-CNT), the results achieved in this article add to the knowledge of voltage stability within CCS voltages under conditions of no-load switching or faults. The findings show that the conventional method of RLC filters can efficiently mitigate transients, with particular emphasis on the fact that this study used a more simplified distribution transformer.

6. Recommendations

The following is the recommendation for future research:

System analysis on the ferroresonance behavior on a CCS using a non-linear distribution transformer needs to be conducted and mitigating factors studied.

Acknowledgements

The author appreciates the ongoing support from Dr. BT Abe and Dr. AF Nnachi of the Tshwane University of Technology.

Conflicts of Interest

The authors declare no conflicts of interest regarding the publication of this paper.

References

[1] Abdel-Hamed, A.M., El-Shafhy, M.M. and Badran, E.A. (2022) High Ohmic Reactor as a Shunt Limiter (HOR-SL) Method for Ferroresonance Elimination in the Distribution System. *IEEE Access*, **10**, 134217-134229. https://doi.org/10.1109/ACCESS.2022.3231190

[2] Abdel-Hamed, A.M., El-Shafhy, M.M. and Badran, E.A. (2023) Investigating Ferro-

resonance in the Distribution Zone. 2022 23*rd International Middle East Power Systems Conference* (*MEPCON*), Cairo, 13-15 December 2022, 1-8. https://doi.org/10.1109/MEPCON55441.2022.10021717

[3] Akpan, U., Essien, M. and Isihak, S. (2013) The Impact of Rural Electrification on Rural Micro-Enterprises in Niger Delta, Nigeria. *Energy for Sustainable Development*, **17**, 504-509. https://doi.org/10.1016/j.esd.2013.06.004

[4] Alghaythi, M.L., Irudayaraj, G.C., Ramu, S.K., Govindaraj, P. and Vairavasundaram, I. (2023) Mathematical Modeling and Analysis of Capacitor Voltage Balancing for Power Converters with Fewer Switches. *Sustainability*, **15**, Article 10698. https://doi.org/10.3390/su151310698

[5] Aminifar, F., Abedini, M., Amraee, T., Jafarian, P., Samimi, M.H. and Shahidehpour, M. (2022) A Review of Power System Protection and Asset Management with Machine Learning Techniques. *Energy Systems*, **13**, 855-892. https://doi.org/10.1007/s12667-021-00448-6

[6] EL-Shafhy, M.M., Abdel-Hamed, A.M. and Badran, E.A. (2022) Ferroresonance in Distribution Systems—State of the Art. *Przeglad Elektrotechniczny*, **98**, 1. https://doi.org/10.15199/48.2022.11.01

[7] Fathi, S.H. and Abbasi, A. (2018) New Technique for Elimination of Ferroresonant Oscillations in Series Capacitor of Power System. *Asian Journal of Scientific Research*, **11**, 203-221. https://doi.org/10.3923/ajsr.2018.203.221

[8] Hepziba, R.J., Balaji, G., Muralikrishma, R. and Rathinavel, S. (2024) A Case Study on Transformer Ferroresonance for Subsea Cable Connected 230kV Substations Using PSCAD. *Electric Power Systems Research*, **230**, Article ID: 110192. https://doi.org/10.1016/j.epsr.2024.110192

[9] Kalair, A., Abas, N., Kalair, A., Saleem, Z. and Khan, N. (2017) Review of Harmonic Analysis, Modeling and Mitigation Techniques. *Renewable and Sustainable Energy Reviews*, **78**, 1152-1187. https://doi.org/10.1016/j.rser.2017.04.121

[10] Kraszewski, W., Syrek, P. and Mitoraj, M. (2022) Methods of Ferroresonance Mitigation in Voltage Transformers in 30kV Power Supply Network. *Energies*, **15**, Article 9516. https://doi.org/10.3390/en15249516

[11] Lin, T.C., Wang, H.H. and Liu, C.H. (2021) Fault Location for Three-Ended Ring-Topology Power System Using Minimum GPS-Based Measurements and CVT/CT Sensing. *IEEE Sensors Journal*, **21**, 22019-22031. https://doi.org/10.1109/JSEN.2021.3100772

[12] Martinez, E., Antonova, G. and Olguin, M. (2013) Ferroresonance Phenomenon in CFE, Its Origin and Effects. 2013 66*th Annual Conference for Protective Relay Engineers*, Texas, 8-11 April 2013, 450-466. https://doi.org/10.1109/CPRE.2013.6822057

[13] Meng, Z., Li, H., Zhang, C., Chen, M. and Chen, Q. (2019) Research on the Reliability of Capacitor Voltage Transformers Calibration Results. *Measurement*, **146**, 770-779. https://doi.org/10.1016/j.measurement.2019.07.011

[14] Navaei, M., Abdoos, A.A. and Shahabi, M. (2018) A New Control Unit for Electronic Ferroresonance Suppression Circuit in Capacitor Voltage Transformers. *International Journal of Electrical Power & Energy Systems*, **99**, 281-289. https://doi.org/10.1016/j.ijepes.2018.01.021

[15] Nene, S.W., Abe, B.T. and Nnachi, A.F. (2023) Modeling and Simulation of a Transmission Line Response to a 400 KV/400V Capacitor Coupled Substation. *Journal of Power and Energy Engineering*, **11**, 1-14. https://doi.org/10.4236/jpee.2023.1112001

[16] Nilsson, S.L., Lima, M. and Young, D.J. (2020) AC Network Control Using Conventional Means. In: Andersen, B. and Nilsson, S., Eds., *Flexible AC Transmission Systems*, Springer, Cham, 51-89. https://doi.org/10.1007/978-3-030-35386-5_3

[17] Nogay, H. S. (2023) Forecasting of Voltage Disturbances at the Beginning of Ferroresonance Phenomena in Power Systems Using by a New Approach of Long-Short Term Memory (LSTM). *Journal of Engineering Research*, **11**, 297-306.

[18] Olanrewaju, E. and Olanrewaju, O. (2020) Rural Electrification and Profitability among Rural Women-Owned Microenterprises in Nigeria. *International Journal of Economics*, **8**, 1-11. https://doi.org/10.34293/economics.v8i4.3381

[19] Pinheiro, P.H., Vidal, M.L., Rocha, F.F. and Fortes, B.W. (2020) Ferroresonance Evaluation on Capacitor Voltage Transformers. *Electrical Engineering*, **102**, 1775-1783. https://doi.org/10.1007/s00202-020-00992-x

[20] Pinheiro, P.H., Vidal, M.L., Rocha, F.F., Franca, B.W. and Fortes, M.Z. (2020) Ferroresonance Evaluation on Capacitor Voltage Transformers. *Electrical Engineering*, **102**, 1775-1783. https://doi.org/10.1007/s00202-020-00992-x

[21] Salihi, J.T. (1960) Theory of Ferroresonance. *Transactions of the American Institute of Electrical Engineers*, *Part I*: *Communication and Electronics*, **87**, 755-763. https://doi.org/10.1109/TCE.1960.6368465

[22] Sanaye-Pasand, M. and Aghazadeh, R. (2003) Capacitive Voltage Substations Ferroresonance Prevention Using Power Electronics Devices. *International Conference on Power Systems Transients*, New Orleans, 28 September-2 October 2003, 1-5.

[23] Saulo, M.J. (2014) Penetration Level of Un-Conventional Rural Electrification Technologies on Power Networks. Ph.D Thesis, University of Cape Town, Cape Town.

[24] Saulo, M.J. and Gaunt, C.T. (2015) The Impact of Capacitor Coupled Sub-Station in Rural Electrification of Sub-Saharan Africa. *International Journal of Energy and Power Engineering*, **4**, 12-29.